

Does Luttinger liquid behaviour survive in an atomic wire on a surface?

L K Dash and A J Fisher

Department of Physics and Astronomy, University College London, Gower Street,
London WC1E 6BT

E-mail: louise.dash@ucl.ac.uk, andrew.fisher@ucl.ac.uk

Abstract. We form a highly simplified model of an atomic wire on a surface by the coupling of two one-dimensional chains, one with electron-electron interactions to represent the wire and one with no electron-electron interactions to represent the surface. We use exact diagonalization techniques to calculate the eigenstates and response functions of our model, in order to determine both the nature of the coupling and to what extent the coupling affects the Luttinger liquid properties we would expect in a purely one-dimensional system. We find that while there are indeed Luttinger liquid indicators present, some residual Fermi liquid characteristics remain.

Submitted to: *J. Phys.: Condens. Matter*

PACS numbers: 71.10.Pm, 73.21.Hb, 79.60.Jv, 81.07.Vb

1. Introduction

A purely one-dimensional metal is not expected to retain the Fermi liquid properties of its three-dimensional counterpart, which is characterized by a one-to-one relationship of its excitations to those of a non-interacting Fermi system and an electron quasiparticle lifetime that diverges to infinity near the Fermi surface. Instead, any interaction between electrons in a one-dimensional metal is expected to lead to a non-zero scattering phase-shift and to destroy completely the quasi-electron nature of the excitations [1]. The resulting “Luttinger liquid” state has separate charge and spin excitations, and quite different transport properties from those of a Fermi liquid. The Luttinger liquid state is an adiabatic continuation of the ground state of a simple one-dimensional model, the Luttinger model [2], in much the same way that a Fermi-liquid state can be adiabatically derived from the ground state of noninteracting fermions.

How could we observe this fascinating state of matter? We cannot fabricate purely one-dimensional systems in the laboratory, but we can produce systems that are quasi-one-dimensional, to a greater or a lesser degree. In several of these, searches for Luttinger liquid behaviour have been undertaken. These include charge-transfer salts such as TMTSF having almost one-dimensional bandstructures [3], semiconductor quantum wires [4], edge states in the quantum Hall effect (which are chiral systems along which electrons can only propagate in one direction) [5, 6], carbon nanotubes [7], and atomic-scale quantum wires fabricated by self-assembly [8] or novel SPM-based surface lithographies [9, 10, 11]. The important question for a theorist is whether such a quasi-one-dimensional system, interacting with a three-dimensional environment, would be expected to show Luttinger liquid behaviour or not, and if so, for what range of parameters. This question was given particular timeliness by the recent angle-resolved photoemission results of Segovia *et al* [8], which have shown that photoemission from chains of Au atoms on Si(111) exhibits features which may be signatures of the spin and charge collective modes indicative of Luttinger liquid behaviour.

In this paper we begin to construct a theoretical framework within which we can answer these questions. We consider the simplest possible model of such a system — one in which the atomic wire is represented by a single-chain spinless Luttinger model, with electron-electron interactions, on a lattice. The environment is represented only by a chain with no interactions but which is otherwise identical. Electrons can hop between the two chains by hybridization of the electron states. Such a simple system does not capture the full complexities of electron scattering with the environment, nor can it represent the magnetic behaviour of a Luttinger liquid. However it provides a relatively simple starting point, and can already be used to calculate one-particle spectral functions such as those probed by photoemission experiments.

In the following sections we explain the details of our model and our numerical methods in Section 2, and then describe our results in Section 3. We find that some aspects of the model display Luttinger liquid-like behaviour while others do not; we then summarize these different properties in Section 4.

2. Theoretical methods

2.1. The Luttinger model

We base our numerical calculations on Haldane's Luttinger model operator method [2] for a chain of spinless idealized atoms with periodic boundary conditions. The Luttinger model is characterized by a linearized dispersion relation with slope v_F and a complete separation of the populations of left- and right-moving particles (as in figure 1) plus the inclusion of an infinity of negative energy electrons [2, 1]. The second of these characteristics makes the model exactly solvable by Haldane's bosonization method, as the boson commutation relations are then exact rather than approximate. The total

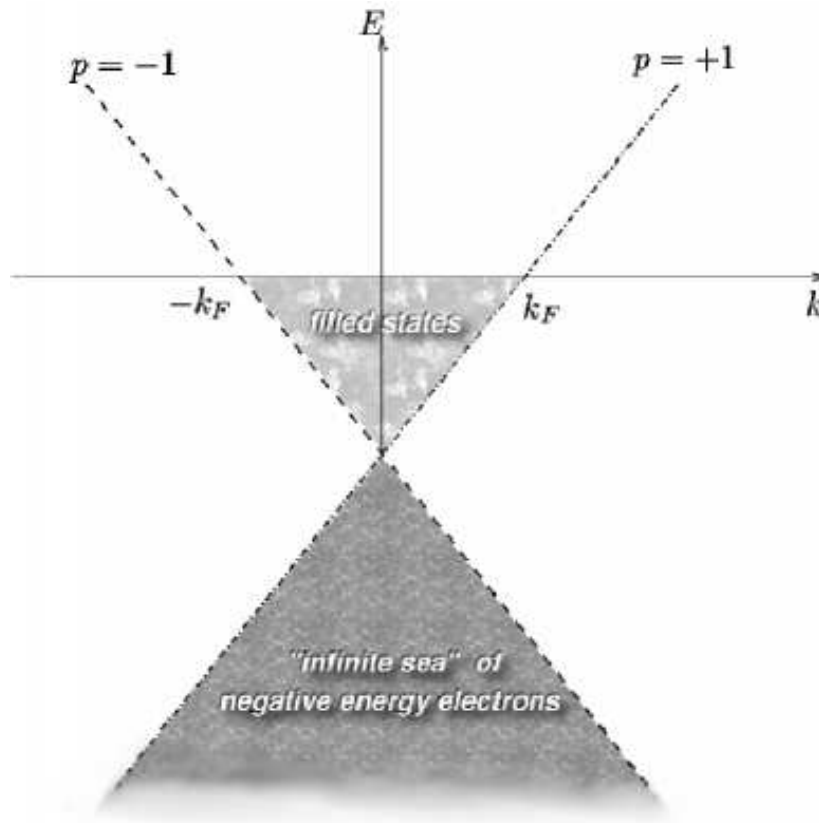


Figure 1. Schematic representation of the Luttinger model. $p = +1, -1$ indicate the populations of left- and right-moving fermions respectively.

Luttinger model Hamiltonian can be split into three parts [1]:

$$\hat{H} = \hat{H}_0 + \hat{H}_2 + \hat{H}_4. \quad (1)$$

\hat{H}_0 represents the non-interacting part of the Hamiltonian:

$$\hat{H}_0 = \sum_{p,k} v_F(pk - k_F) : \hat{c}_{pk}^\dagger \hat{c}_{pk} :, \quad (2)$$

where q indicates momentum and p ($= \pm 1$) the branch index for the left- (-1) and right-moving ($+1$) fermions. The operator \hat{c}_{pk}^\dagger creates a fermion of type p with momentum k

and $:\dots:$ implies normal ordering. The interaction parts of the Hamiltonian, \hat{H}_2 and \hat{H}_4 , are given respectively by

$$\hat{H}_2 = \frac{2}{L} \sum_q g_2(q) \hat{\rho}_+(q) \hat{\rho}_-(-q), \quad (3)$$

$$\hat{H}_4 = \frac{1}{L} \sum_{p,q} g_4(q) \hat{\rho}_p(q) \hat{\rho}_p(-q). \quad (4)$$

The \hat{H}_2 term represents forward scattering between the left- and right-moving fermion branches, while the \hat{H}_4 term represents forward scattering within a momentum branch. Note however that $[\hat{H}_2, \hat{H}_0] \neq 0$, so \hat{H}_2 can modify the ground state by excitation of particle-hole pairs, whereas \hat{H}_4 commutes with \hat{H}_0 and so cannot modify the ground state. The density operators $\hat{\rho}$ are defined in terms of the fermion operators as

$$\hat{\rho}_p(q) = \sum_k : \hat{c}_{p,k+q}^\dagger \hat{c}_{p,k} : = \sum_k \left(\hat{c}_{p,k+q}^\dagger \hat{c}_{p,k} - \delta_{q,0} \langle \hat{c}_{p,k}^\dagger \hat{c}_{p,k} \rangle_0 \right). \quad (5)$$

The complete Hamiltonian can be diagonalized via a Bogoliubov transformation [2] to yield the bosonized form of the Hamiltonian

$$\tilde{H} = \frac{\pi}{L} \sum_{p, q \neq 0} v_0(q) : \tilde{\rho}_p(q) \tilde{\rho}_p(-q) : + \frac{\pi}{2L} [v_N (N_+ + N_-)^2 + v_J (N_+ - N_-)^2] \quad (6)$$

$$= \frac{1}{2} \sum_q (\omega_q - v_F |q|) + \sum_q \omega_q \hat{b}_q^\dagger \hat{b}_q + \frac{\pi}{2L} (v_N N^2 + v_J J^2), \quad (7)$$

where the transformed density operators $\tilde{\rho}$ are related to the originals by a phase ϕ_q :

$$\tilde{\rho}_p(q) = \hat{\rho}_p(q) \cosh \phi_q + \hat{\rho}_{-p}(q) \sinh \phi_q. \quad (8)$$

There is a characteristic frequency $\omega_q = |(v_F + g_4(q)/2\pi)^2 - (g_2(q)/2\pi)^2|^{1/2}/|q|$ associated with the transformed bosons, while the quantum numbers $N \equiv N_+ + N_-$ and $J \equiv N_+ - N_-$ represent respectively the sum of the number of electrons on the positive and negative branches, and the difference between them (analogous to current).

The three velocities in the Hamiltonian are related as follows:

$$\begin{aligned} v_N v_J &= v_0^2, \\ v_N &= \frac{v_0}{K_\rho} = v_0 e^{-2\phi}, \\ v_J &= v_0 K_\rho = v_0 e^{+2\phi}, \end{aligned} \quad (9)$$

and are also related to the non-interacting Fermi velocity by

$$\begin{aligned} v_N &= v_F + \frac{g_4 + g_2}{2\pi}, \\ v_J &= v_F + \frac{g_4 - g_2}{2\pi}. \end{aligned} \quad (10)$$

The requirement that \tilde{H} be a diagonalized version of \hat{H} is ensured by the relationship between the Bogoliubov transformation phase ϕ_q and the interaction functions g_i :

$$e^{2\phi_q} = \left(\frac{\pi v_F + g_4(q) - g_2(q)}{\pi v_F + g_4(q) + g_2(q)} \right)^{1/2} \quad (11)$$

$$\equiv K_\rho(q). \quad (12)$$

The spinless Luttinger liquid parameter K_ρ is then obtained by taking the limit of $K_\rho(q)$ as q tends to zero. In all of the above the limit $q \rightarrow 0$ is implied where q is not explicitly included.

In addition there are two further parameters related to K_ρ : for a spinless Luttinger liquid they are given by

$$\alpha = \frac{1}{2} \left[K_\rho + \frac{1}{K_\rho} - 2 \right], \quad (13)$$

$$\gamma = 2\alpha. \quad (14)$$

The Fermi liquid corresponds to $K_\rho = 1$ and $\alpha = 0$ and so departures from these values can be used to “measure” the extent of non-Fermi liquid behaviour. α is an exponent which governs the power-law dependence of all single-particle properties (for example the density of states, which varies as $N(E) \approx |E - E_F|^\alpha$), as well as other properties of the system, including the d.c. resistivity, which varies as $\rho(T) \approx T^{1-\gamma}$ [1, 12].

2.2. Coupling two chains

We are now able to couple two Luttinger chains (labelled by superscript A and B) together by allowing hopping between adjacent points on each chain with matrix element t_\perp :

$$\hat{H}^{\text{coupled}} = \hat{H}^A + \hat{H}^B + t_\perp \sum_{x,p} \left(\hat{\psi}_p^{A\dagger}(x) \hat{\psi}_p^B(x) + \hat{\psi}_p^{B\dagger}(x) \hat{\psi}_p^A(x) \right). \quad (15)$$

Other schemes of inter-chain hopping are of course possible, and we expect that they will generate similar results. We neglect any “drag effects” of inter-chain interactions that would be generated by interaction terms analogous to \hat{H}_2 or \hat{H}_4 involving electrons on both chains. We have the choice of using either a set of basis states generated by the diagonalized boson operators \hat{b}_q^\dagger or the non-diagonalized operators \hat{a}_q^\dagger . We choose the latter, as although this has the consequence that the ground states for a single interacting chain no longer consist of the relevant zero-boson basis states, it is considerably more convenient computationally. $\hat{\psi}^\dagger$ are fermion creation operators given in the bosonized form by

$$\hat{\psi}_{p,c}^\dagger(x) = \frac{1}{\sqrt{L}} e^{ipk_F x} \left[e^{i\hat{\phi}_p^\dagger(x)} \hat{U}_{p,c} e^{i\hat{\phi}_p(x)} \right], \quad (16)$$

$\hat{\phi}_p(x)$ is a boson field operator given by

$$\hat{\phi}_p(x) = \left(\frac{p\pi x}{L} \right) N_p + i \sum_{q \neq 0} \theta(pq) \left(\frac{2\pi}{L|q|} \right)^{1/2} e^{iqx} \hat{a}_q, \quad (17)$$

where the subscript p refers to the branch index (± 1) and c to the chain index. $\hat{U}_{p,c}$ is a ladder operator whose form ensures the anticommutation properties of the final fermion operator $\hat{\psi}_p^\dagger(x)$ despite the commutation properties of the constituent boson operators \hat{a}_q .

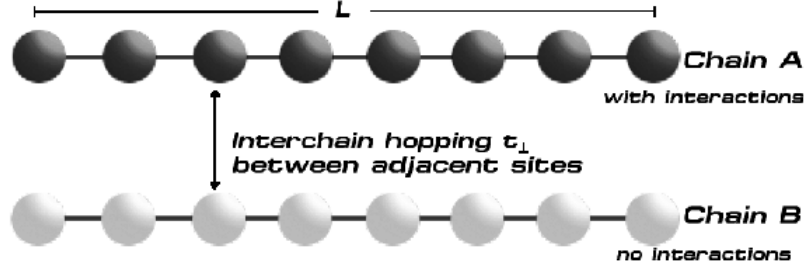


Figure 2. Representation of the two chains. Electron-electron interactions are included on just one of the chains.

In order for $\hat{U}_{p,c}$ to produce anticommuting field operators on different chains, it is necessary to introduce a further phase factor into its definition, analogous to Haldane’s phase factor $\zeta(p, N_p, N_{-p})$ for ensuring anticommutation between the branches of a single chain. The total ladder operator component of equation (16) thus takes the form

$$\hat{U}_{p,c} = \zeta(p, N_p, N_{-p}) \zeta'(c, N_c, N_{-c}) |N_{p,c} + 1, N_{-p,c}\rangle, \quad (18)$$

where the subscript $c = \pm 1$ is a chain index. The anticommutation properties originate in the phase factors ζ , which can be written as

$$\zeta_{i=p,c} = (-1)^{(\frac{1}{2}iN_{-i})}. \quad (19)$$

2.3. Computational details

The choice of a specific form for the interactions $g_2(q)$ and $g_4(q)$ is arbitrary, as the Luttinger liquid remains completely solvable for any interaction that fulfils certain conditions [2]. We choose a Gaussian form for the interaction and set $g_2(q) = g_4(q) = 2\pi V(q)$ with

$$V(q) = I \exp(-2q^2/r) \quad (20)$$

as this has the advantage that it maintains the same form in both real and momentum space. Other forms, such as a screened Coulomb interaction, would also be possible. The parameter I can be varied to control the “strength” of the interaction, and r controls the range of the interactions.

Our model is completed by setting the interaction strength on chain B to zero but retaining interactions on chain A. With the non-interacting chain representing the surface and the interacting chain the wire, we therefore form our highly simplified model of an atomic wire interacting with a substrate.

The size of the computational Hilbert space is restricted by allowing only one boson in each mode. While this successfully truncates the Hilbert space to a manageable size it does not affect the low energy properties in which we are interested, as we have checked that only higher energy excitations involve basis states with more than one boson in each mode. We also neglect the presence of the infinity of negative energy electrons,

i.e. $\hat{c}|N_{\text{electrons}} = 0\rangle = 0$. However, we are still strongly limited in the size of the system we can handle: the Hilbert space scales exponentially with both length of chains and number of electrons. The largest system for which we have been able to calculate with arbitrary numbers of electrons is one with length $L = 6$ (i.e. 12 sites in total). In order to obtain both the eigenstates of the coupled system and its correlation functions we utilize the Lanczos method [13, 14].

2.4. Spectral functions

We define the spectral function $\rho(q, \omega)$ as

$$\rho(q, \omega)_{p,c} = -\frac{1}{\pi} \Im [G_{p,c}^R(k_F + q, \omega + \mu)] , \quad (21)$$

with $q = k_F - k$, and the retarded Green's function $G_{p,c}^R$ defined as the double Fourier transform of

$$G_{p,c}^R(x, t) = -i\theta(t) \{ \langle \hat{\psi}_{p,c}(x, t) \hat{\psi}_{p,c}^\dagger(0, 0) \rangle \} \quad (22)$$

where the subscripts p and c again indicate branch and chain indices. It is possible to derive an analytic form for the spectral function of a single Luttinger liquid, either with or without spin, as in references [15, 16, 17]. Whereas for a Fermi liquid we would expect $\rho(0, \omega)$ to be a delta function at the Fermi energy, the situation for a Luttinger liquid is quite different. Spectral weight is repelled from the Fermi surface owing to the virtual particle-hole excitations generated by the inter-branch scattering term g_2 , resulting in a broadened peak. As q is increased the Fermi liquid spectral function will merely broaden like q^2 reflecting the finite lifetime of electrons away from E_F , but for a Luttinger liquid there is zero spectral weight within a range $\pm v_0 q$ of the Fermi energy. In addition, the negative frequency contribution is suppressed exponentially with q , and for a continuum Luttinger liquid the positive frequency contributions have a power law dependence. For $\omega > 0$ this is of the form $\theta(\omega - v_0 q)(\omega - v_0 q)^{\gamma-1}$ and for $\omega < 0$ it is of the form $\theta(-\omega - v_0 q)(-\omega - v_0 q)^\gamma$, with γ given by equation (14) [1].

However, for our more complex system it is not easy to obtain an analytic form and so we resort to computational methods. We calculate the Green's function

$$G^R(k, k', \omega) = \langle N | \hat{c}_k \left[\omega - \hat{H} + \varepsilon_N \right]^{-1} \hat{c}_{k'}^\dagger | N \rangle + \langle N | \hat{c}_{k'}^\dagger \left[\omega + \hat{H} - \varepsilon_N \right]^{-1} \hat{c}_k | N \rangle \quad (23)$$

using Haydock's tridiagonal Lanczos-based procedure [13]. In order to ensure convergence, we put $\omega \rightarrow \omega + i\eta$, where η is an imaginary component of the energy roughly equal to the level spacing of the system [13]. $|N\rangle$ is the N -electron ground state, with energy ε_N .

3. Results

In this section we present our numerical results, concentrating on $L = 6$ (our largest system). The results for $L = 4$ are very similar, and this encourages us to believe that, despite the small size of our system, finite-size effects are not dominating the results. All results shown here were calculated with $v_F = 1$.

3.1. Ground and excited states

The ground and neutral first excited states are calculated for different values of the interaction strength I as detailed above. As we have chosen the basis states for the system to be those before the Bogoliubov transformation, we find that the non-interacting ground state (i.e. $I = 0$) consists entirely of zero-boson basis states, whereas all the interacting systems ($I > 0$) have contributions from basis states that include bosons on one or both chains, as these basis states are not individually eigenstates of the interacting system. The contribution to the ground states from basis states containing either no bosons on either chain, bosons on the chain with explicit interactions only (i.e. chain A) and bosons on both chains are shown in figure 3.

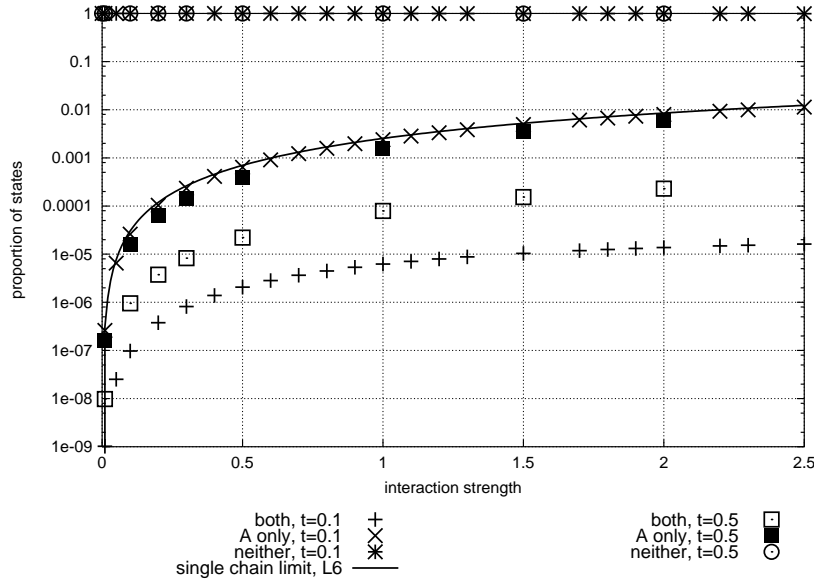


Figure 3. Contribution of bosonic basis states to the ground states of the $L = 6$, $N = 2$, $t_{\perp} = 0.1$ and $L = 6$, $N = 2$, $t_{\perp} = 0.5$ systems as a function of interaction strength I . See text for a full explanation.

The corresponding data for the boson contributions to a single isolated Luttinger liquid chain with otherwise identical parameters is also shown in figure 3. This matches almost exactly the contribution for the system's interacting chain (chain A) and thus indicates we are in a regime where the two chains can be said to be weakly coupled for both coupling strengths $t_{\perp} = 0.1$ and 0.5 .

The energies of the ground and first excited states are plotted in figure 4. We see that the ground state energy has a region of roughly linear dependence on I in the range $0 \lesssim I \lesssim 0.5$ and thereafter is rather less dependent on I . The first excited state, however, is linear in I for $I \lesssim 2$, at which point it becomes completely independent of I . The excitation energy ΔE for the non-interacting system is equal to $2t_{\perp}$, indicating that for this size of system the first excitation is one between the bonding and anti-bonding bands with zero net momentum change. As we increase I however, the bonding and

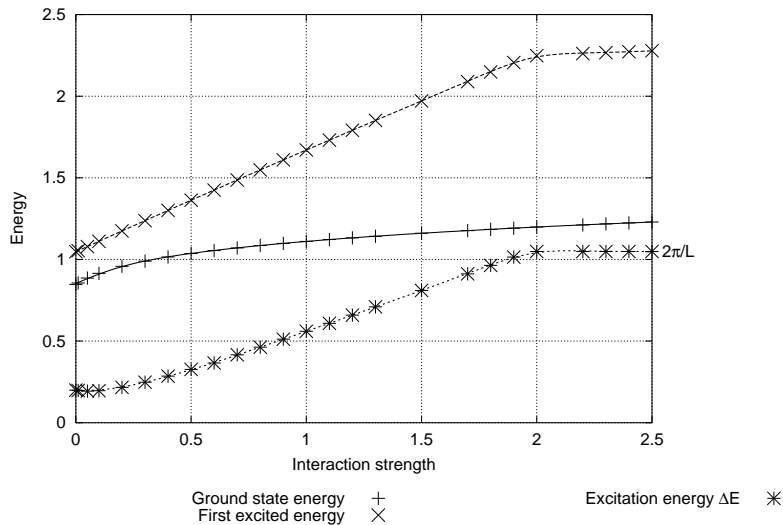


Figure 4. Energies for the ground state and neutral first excited state for the $L = 6$, $N = 2$, $t_{\perp} = 0.1$ system as a function of interaction strength I .

antibonding bands distort to such an extent that eventually, at $I \approx 2.0$, the lowest excitation becomes not one between bands with zero net momentum, but an intra-band one with net momentum change $2\pi v/L$. For a Luttinger liquid, we would expect the velocity v in this expression to be the Luttinger velocity v_0 (as in equations (9), etc.) rather than the Fermi velocity v_F , leading to a continued I -dependence for ΔE . However, it is clear from figure 4 that this is not the case for this system: the excitation energy for $I \gtrsim 2.0$ remains constant and equal to $2\pi v_F/L = \pi/3$. (For this system $v_F = 1$.) This can be explained as follows — as I is increased the single-chain energy levels on chain A increase (since the interaction is repulsive), while those on the non-interacting chain B remain constant. It therefore becomes energetically preferable for the electrons to move to the non-interacting chain B rather than remain on the (interacting) chain A, until the point is reached at which the system is predominantly populated by electrons on chain B. This chain is still Fermi liquid-like, thus shifting the properties of the system as a whole back from partially Luttinger liquid-like to Fermi liquid-like.

This is confirmed by an examination of the location of the electrons for both the ground and first excited states. Figure 5 shows a plot for $L = 6, N = 2, t_{\perp} = 0.1$, showing the chain to which the electrons “belong”, again based on an analysis of the contribution of each of the basis states forming the eigenstate. As we have only 2 electrons in this system, there are three possible distributions for the electrons: both on chain A (“A-like”), both on chain B (“B-like”) or one on each chain (“equal”).

First consider the ground states. We see that for the non-interacting ground state the electrons are distributed equally between the chains, and once interactions are switched on we evolve continuously towards a regime where basis states with electrons on chain A are strongly suppressed in favour of states with both electrons on chain B.

The situation for the excited states is however quite different. We start at $I = 0$

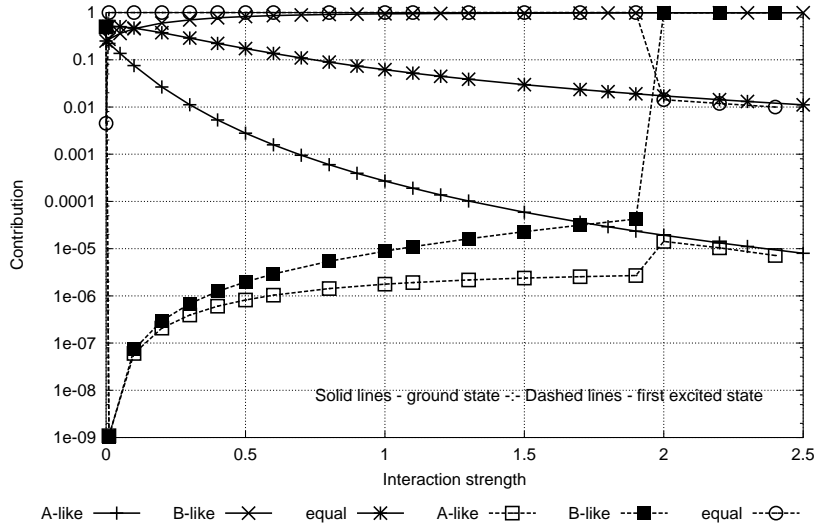


Figure 5. Contributions to the ground and first excited states for the $L = 6$, $N = 2$, $t_{\perp} = 0.1$ system from electrons on each chain as a function of interaction strength I . See text for a full explanation.

with a state in which, like the ground state, the electrons are equally distributed between the chains. This state is, however, 4-fold degenerate and immediately even weak interactions are introduced, this degeneracy is lifted and, in what is now the lowest state, the contribution from basis states with both electrons on the same chain are strongly suppressed. The first excited state for small values of I may therefore be thought of as “covalent” in nature, as opposed to the “ionic”-like states that contribute to the non-interacting state where both electrons are on the same chain. As interactions are increased further, the contribution from the ionic-like states begins to return. However, once we hit the point (at $I = 2.0$) where the nature of the excitations changes from zero net momentum change to $\Delta k = 2\pi v_F/L$, there is once more a discontinuity in the plot and the electron contributions from this point match those of the ground state, indicating that there is no net interchain electron hopping involved in these excitations.

3.2. Spectral functions

Results from the calculation of the spectral function $\rho(q = 0, \omega)$ are presented in figure 6. There are three sources of the broadening of the peaks away from the delta function one would expect from a Fermi liquid. The first of these is due to the finite value of the imaginary energy η we have used in our calculations, leading to broadening of the peaks into Lorentzians with width $\sim \eta$. The second results from the splitting into bonding and anti-bonding bands due to the inter-chain coupling and is equal to $2t_{\perp}$. The remaining broadening, however, is due to the removal of spectral weight from the Fermi energy at $\omega = 0$, and is indicative of Luttinger liquid behaviour in the coupled system.

We can also calculate $\rho(q \neq 0, \omega)$ although for our extremely small system, we are severely restricted in available values of q . As we would expect for a Luttinger

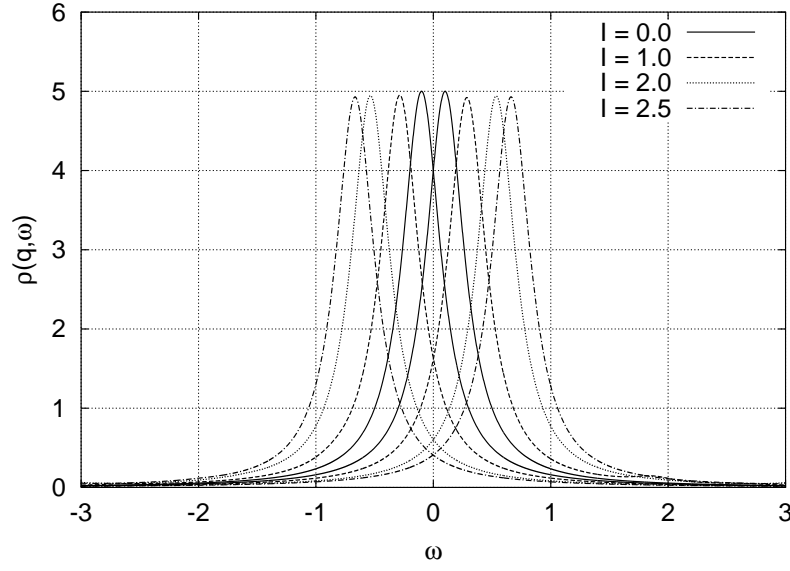


Figure 6. Hole (left peak) and electron (right peak) contributions to the spectral function $\rho(q = 0, \omega)$. $t_{\perp} = 0.1$, $\eta = 2t_{\perp}$. In order to show the splitting clearly, the electron and hole contributions are shown as equal in magnitude.

liquid, there is a strong suppression of the hole contribution for $q > 0$. Owing to the discrete nature of this system, it is not possible to calculate the Luttinger parameter K_{ρ} direct from the slopes of the electron and hole contributions as in references [15, 16, 17]. However, we can still derive a value for K_{ρ} from the separation of the electron and hole peaks as follows: For a non-interacting coupled chain system, the electron and hole contributions to $\rho(q = 0, \omega)$ are separated by $2t_{\perp}$, whereas for a single Luttinger liquid the contributions to $\rho(q \neq 0, \omega)$ are separated by $2v_0q$. We define an effective v_0 in terms of the peak splitting $\Delta\omega$ by the relation

$$\Delta\omega = 2(v_0^{\text{eff}}q + t_{\perp}). \quad (24)$$

Then, since we have $g_2(q) = g_4(q)$, we can use v_0^{eff} as a measure of v_0 and equate equations (9) and (10) to give an expression for the Luttinger parameter:

$$K_{\rho}^{-1} = e^{-2\phi} = \frac{1}{v_0^{\text{eff}}} \left[v_F + \frac{(v_0^{\text{eff}2} - v_F^2)}{v_F} \right] \quad (25)$$

$$= v_0^{\text{eff}}, \quad (26)$$

since $v_F = 1$. The results of this calculation and the corresponding values of the parameter α (equation (13)) are plotted in figure 7.

4. Conclusions

Our calculations approach the question of whether our model exhibits Luttinger liquid behaviour from several complementary directions. We have presented results for the

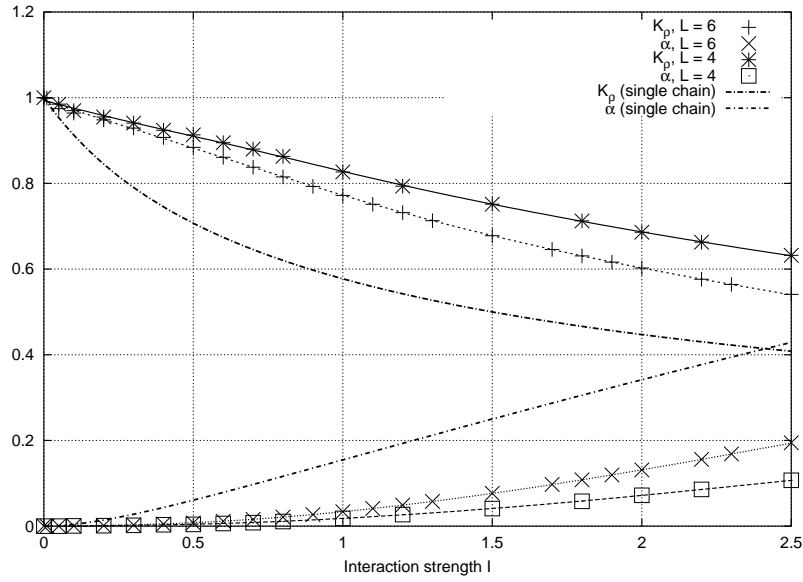


Figure 7. Luttinger parameters K_ρ and α for the coupled chain system, both $L = 6$ and $L = 4$, and for an isolated continuum limit ($L \rightarrow \infty$) chain.

nature of the ground state, for the nature of excited states (charged and neutral) and the related response functions governing the response of the system to excitation. We have also estimated the exponents in certain power-laws characterizing the Luttinger liquid state.

Our results display a certain ambiguity with regard to whether or not this system is a Luttinger liquid. Roughly speaking, the evidence from the bosonic nature of the ground state, the charged excited states, and the values of the scaling parameters is all broadly consistent with Luttinger liquid behaviour, modified by the presence of the second chain.

Specifically, the one-particle spectral function is consistent with Luttinger liquid behaviour. At $q = 0$, the total spectral function is broadened by separation of the electron and hole parts—this separation is much greater than the $2t_\perp$ expected in a non-interacting two-chain system. For $q \neq 0$, there is additional separation of the electron and hole parts, consistent with the further suppression of spectral weight near the Fermi energy. (For $q > 0$, corresponding to probing the occupancy of states with $k > k_F$ — see equation (21) — the hole part of the spectral function is strongly suppressed, even for relatively strong interactions.) Further support for the Luttinger liquid hypothesis comes from the composition of that portion of the ground state in which bosons are excited on chain A: this fraction closely tracks the fraction that would be expected in an isolated single-chain Luttinger liquid (Figure 3).

Moreover, we are able to derive indirectly from $\rho(q > 0, \omega)$ values for two Luttinger liquid parameters: K_ρ (which determines the ratio of the different velocities) and α (which determines the asymptotic behaviour of the correlation functions). Although our analysis presupposes the validity of relations characterizing the Luttinger liquid

state (equation (25)), the results are self-consistent in the sense that they show $K_\rho < 1$ and $\alpha > 0$, i.e., departures from the Fermi-liquid values. The degree of departure from Fermi-liquid values is, however, somewhat less than would be expected for a single-chain system with the same interaction strength (see Figure 7).

However, we also have evidence that there is some residual Fermi liquid behaviour. This comes principally from the distribution of charge across the two chains, as a function of interaction strength, in the ground and neutral excited states. Transfer of charge to the non-interacting chain at higher values of I results in the resurrection of a Fermi-liquid like neutral excitation spectrum (although we are still able to extract non-Fermi liquid values for the Luttinger parameters for these interaction strengths, as explained above).

This implies that while the neutral excitation spectrum undergoes a transformation to Fermi liquid behaviour at large I , the charged excitation spectrum does not. It remains to be seen how the apparent conflict between these different views on the same underlying quantum state is resolved.

Finally, it should be noted that in our system the surface is represented as metallic, although in order to achieve true one-dimensional conduction in an experiment it is much more likely that a semiconducting or insulating substrate would be employed, as in the work of [8]. One might expect that with a gapped substrate, the elimination of hybridization with substrate states at the Fermi energy would promote Luttinger liquid formation by comparison with the metallic case. So our finding that some aspects of Luttinger liquid spectral behaviour persist even in the metallic case may also have implications for recent and future experiments. We plan further theoretical work on semiconducting substrates. It would also be interesting to study the influence of wire-substrate interactions other than simple hybridization on Luttinger liquid formation.

Acknowledgments

LKD thanks EPSRC and the National Physical Laboratory for support in the form of a CASE studentship; AJF thanks EPSRC for the award of an Advanced Fellowship.

- [1] Voit J, 1995 *Reports on Progress in Physics* **58** 977
- [2] Haldane F, 1981 *Journal of Physics C* **14** 2585
- [3] Schwartz A *et al.*, 1998 *Physical Review B* **58** 1261
- [4] Wang D *et al.*, 2000 *Physical Review Letters* **85** 4570
- [5] Wen X, 1990 *Physical Review B* **41** 12,838
- [6] Chang A *et al.*, 1996 *Physical Review Letters* **77** 2538
- [7] Bockrath M *et al.*, 1999 *Nature* **397** 598
- [8] Segovia P *et al.*, 1999 *Nature* **402** 504
- [9] Watanabe S *et al.*, 1997 *Surface Science* **386** 340
- [10] Yajima A *et al.*, 1999 *Physical Review B* **60** 1456
- [11] Hitosugi T *et al.*, 1999 *Physical Review Letters* **82** 4034
- [12] Ogata M and Anderson P, 1993 *Physical Review Letters* **70** 3087
- [13] Haydock R, 1980 *Solid State Physics* **35** 215

- [14] Golub G H and van Loan C F, 1996 *Matrix Computations* (Baltimore: Johns Hopkins University Press), 3rd ed.
- [15] Schönhammer K and Meden V, 1993 *Physical Review B* **47** 16,205
- [16] Voit J, 1993 *Journal of Physics C* **5** 8305
- [17] Meden V and Schönhammer K, 1992 *Physical Review B* **46** 15,753